ICIC Express Letters ICIC International ©2022 ISSN 1881-803X
Volume **16**, Number **9**, September **2022** pp. **957–964**

A COMPARISON OF CONTROL STRATEGIES FOR HYBRID ACTIVE POWER FILTER

Chau Minh Thuyen* and Nguyen Duc Toan

Faculty of Electrical Engineering Technology
Industrial University of Ho Chi Minh City
No. 12, Nguyen Van Bao, 4 Ward, Go Vap District, Ho Chi Minh City 700000, Vietnam
nguyenductoan@iuh.edu.vn
*Corresponding author: chauminhthuyen@iuh.edu.vn

Received November 2021; accepted January 2022

Abstract. *This paper proposes a comparison of control strategies for Hybrid Active Power Filter (HAPF). First, the mathematical model of HAPF was established. Based on the mathematical model, the analysis of the control strategies for HAPF has been performed. Accordingly, the control strategy based on the supply harmonic current and the load harmonic current is equally effective, regardless of the influence of the source distortion. However, when the source is distorted, the control strategy based on source harmonic current will be more efficient than the control strategy based on the load harmonic in eliminating harmonics in the supply current and avoiding resonance between the impedances of the passive power filters with the system impedance. The simulation results have compared the effectiveness of the two above control strategies.*
Keywords: Hybrid active power filter, Control strategy, Harmonic filter, Passive power filter

1. **Introduction.** Currently, the Hybrid Active Power Filter (HAPF) is playing a very important role in harmonic filtering and reactive power compensation in the power system [1-4]. HAPF is a hybrid form of Active Power Filter (APF) [5] and Passive Power Filters (PPFs), the PPFs in HAPF systems are usually designed to suppress high order harmonic components, while low order harmonics will be handled by APF. This hybrid structure reduces the capacity of the APF circuit, resulting in a low initial investment cost and it can be used for high voltage grids and large capacity load.

Until now, there are many studies on HAPF and these researches mainly focus on the following directions: parameters multi-objective optimization of HAPF [6-8], stabilization of DC bus voltage of inverter [9-11], using Hysteresis [12,13], PI [14-16], fuzzy [17,18], hybrid fuzzy [19,20], neural fuzzy [21-23] controllers, and structural improvement of the HAPF [24,25]. However, the above published control studies for HAPF sometimes use a control strategy based on the load harmonic current [2,3,6-8,19,20], and sometimes use a control strategy based on the supply harmonic current [5,10,11,14]. In addition, the research results only focus on considering the influence of the harmonic current component from the load, not considering the influence of the harmonic component from the source. In practice, the three-phase mains voltage is not always ideal. If the three-phase supply voltage is distorted, what control strategy is effective? To clarify the above problem, this paper performs a mathematical model analysis of HAPF to find out the relationship between the supply current and other parameters in the HAPF system. Accordingly, the influence of the harmonic source voltage and the harmonic current of the load on the supply current is very significant. When three-phase source voltage is ideal, the effect of the two above control strategies is the same. However, when the three-phase source

DOI: 10.24507/icicel.16.09.957

voltage has harmonic distortion, the control strategy based on the source harmonic current proves to be more effective. The simulation results have demonstrated the effectiveness of the two above control strategies.

This paper is structured into 4 parts: Part 1 presents the importance of the problem to be researched, the mathematical model and analysis of control strategy for HAPF are presented in Part 2, Part 3 shows the simulation results and comments, Part 4 gives the conclusion of the paper.

2. **Mathematical Model and Analysis of Control Strategy for HAPF.** The model of HAPF is shown in Figure 1, where u_s and Z_s are voltage and impedance of the source, C_F is injected capacitance, C_1 and L_1 are the resonant capacitance and inductance at the fundamental frequency, C_P and L_P are the resonant capacitance and inductance at the 11th and 13th, L_0 is the inductance of the output filter, V_{dc} is the DC bus voltage of the inverter, load modeled by balanced load L_L-R_L and harmonic sources 5th, 7th, 11th, 13th.

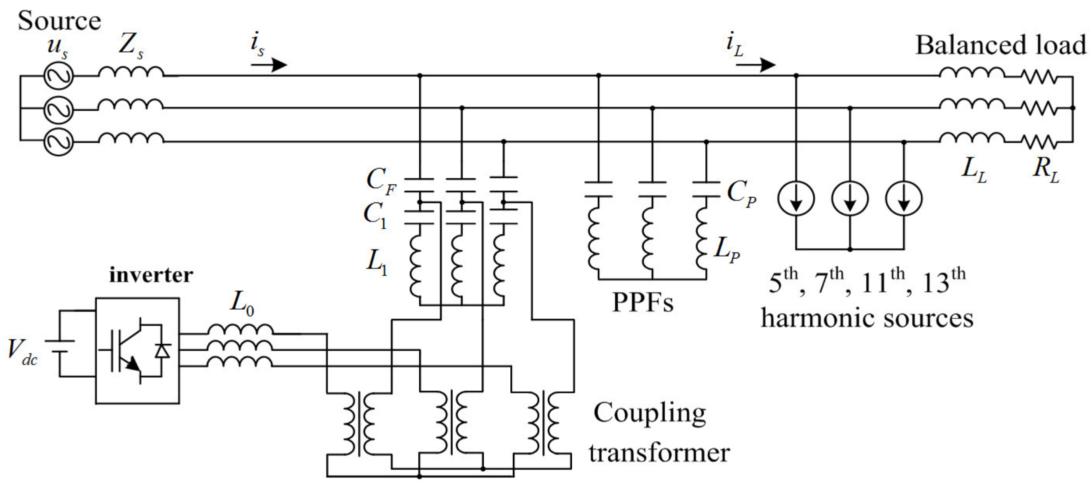

FIGURE 1. Model of HAPF

The single-phase equivalent circuit when considering the influence of the harmonic source is shown in Figure 2.

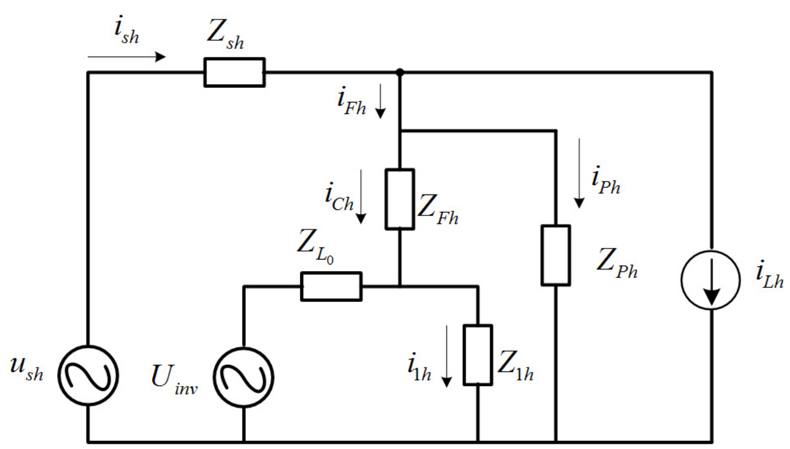

FIGURE 2. Single-phase equivalent circuit when considering the effect of harmonics

Because L_0 has a small value, its impedance is also small. From Figure 2, u_{sh} is written as

$$u_{sh} = i_{sh}Z_{sh} + i_{Ch}Z_{Fh} + U_{inv} \tag{1}$$

On the other hand

$$i_{sh} = i_{Lh} + i_{Ch} + i_{Ph} \tag{2}$$

$$u_{sh} = i_{sh}Z_{sh} + i_{Ph}Z_{Ph} \tag{3}$$

From here, the control strategies for HAPF are analyzed as follows:

+*Control strategy based on load harmonic current:* $U_{inv} = K_1 i_{Lh}$

where K_1 is a controllable factor that depends on the transfer function of the controller used, the transfer function of the inverter, and the transfer function of the output circuit (from the output of the inverter to the point connected with the grid).

Equation (1) can be rewritten as

$$u_{sh} = i_{sh}Z_{sh} + i_{Ch}Z_{Fh} + K_1 i_{Lh} \tag{4}$$

From (2), i_{Ch} is written as

$$i_{Ch} = i_{sh} - (i_{Lh} + i_{Ph}) \tag{5}$$

Substituting (5) into (4):

$$\begin{aligned} u_{sh} &= K_1 i_{Lh} + Z_{Fh}\left[i_{sh} - i_{Lh} - i_{Ph}\right] + i_{sh}Z_{sh} \\ &= i_{sh}\left(Z_{Fh} + Z_{sh}\right) - Z_{Fh}i_{Lh} - Z_{Fh}i_{Ph} + K_1 i_{Lh} \end{aligned} \tag{6}$$

The supply harmonic current will be

$$i_{sh} = \frac{\left(Z_{Fh} - K_1\right) i_{Lh}}{Z_{Fh} + Z_{sh}} + \frac{Z_{Fh}}{Z_{sh} + Z_{Fh}} i_{Ph} + \frac{u_{sh}}{Z_{sh} + Z_{Fh}} \tag{7}$$

Substituting $i_{Ph} = \frac{u_{sh} - i_{sh}Z_{sh}}{Z_{Ph}}$ into (7):

$$i_{sh} = \frac{\left(Z_{Fh} - K_1\right) Z_{Ph}}{Z_{Ph}Z_{sh} + Z_{Ph}Z_{Fh} + Z_{Fh}Z_{sh}} i_{Lh} + \frac{\left(Z_{sh} + Z_{Fh}\right)}{Z_{Ph}Z_{sh} + Z_{Ph}Z_{Fh} + Z_{Fh}Z_{sh}} u_{sh} \tag{8}$$

Setting $Z' = \frac{Z_{Ph}Z_{Fh}}{Z_{Ph} + Z_{Fh}}$, the equation describing the supply harmonic current would be

$$i_{sh} = \frac{Z'\left(Z_{Fh} - K_1\right)}{Z_{Fh}\left(Z_{sh} + Z'\right)} i_{Lh} + \frac{1}{Z_{sh} + Z'} u_{sh} \tag{9}$$

Equation (9) shows that if the harmonic component of the source voltage is not taken into account ($u_{sh} = 0$), when K_1 is large enough, the supply harmonic current will be greatly reduced. However, the possibility of resonance between the impedances Z_{Ph}, Z_{Fh}, Z_{sh} is possible. This is very dangerous. If the source voltage has harmonic components ($u_{sh} \neq 0$), then this control strategy is not effective even if the value K_1 is large enough.

+*Control strategy based on supply harmonic current:* $U_{inv} = K_2 i_{sh}$

Proving similarly, we get

$$i_{sh} = \frac{u_{sh} i_{Lh}}{K_2 + Z_{sh} + 2Z_{Fh}} + \frac{Z_{Fh} + u_{sh}}{K_2 + Z_{Fh} + 2Z_{sh}} i_{Lh} + \frac{Z_{Fh}}{Z_{Ph}\left(K_2 + Z_{sh} + 2Z_{Fh}\right)} \tag{10}$$

where K_2 is a controllable factor, and it depends on the transfer function of the controller used and the transfer function of the inverter.

Equation (10) shows that if the harmonic component of the source is not taken into account ($u_{sh} = 0$), when K_2 large enough, the harmonic component of the supply current will be reduced to the lowest level. Besides, the resonance between the impedances Z_{Ph}, Z_{Fh}, Z_{sh} will not be possible. If the source has harmonic components ($u_{sh} \neq 0$), this control strategy is also effective if K_2 is large enough.

3. **Simulation Results and Discussion.** To demonstrate the effectiveness of control strategy based on load harmonic currents and supply harmonic currents, simulation results were performed on a 10 kV-50 Hz HAPF system with the following parameters: $C_F = 50$ μF, $C_1 = 228.47$ μF, $L_1 = 44.34$ mH, $L_0 = 0.1$ mH, $V_{dc} = 600$ V, $R_L = 15$ Ω, $L_L = 60$

mH. PPFs are designed to cancel harmonics 11th and 13th with values of $C_{11} = 22.2$ µF, $L_{11} = 3.77$ mH, $C_{13} = 22.2$ µF, $L_{13} = 2.7$ mH. The harmonic sources are modeled by four harmonic current sources 5th, 7th, 11th and 13th with amplitudes of 37 A, 30 A, 27 A, and 22 A, respectively.

The simulation is performed on two modes of HAPF: when the source voltage is undistorted and when the source voltage is distorted.

When the source voltage is undistorted, a control strategy based on the load harmonic current and a control strategy based on the supply harmonic current give results as the same. Simulation results and frequency spectrum of waveforms with the control strategy $U_{inv} = K_1 i_{Lh}$ or $U_{inv} = K_2 i_{sh}$ are shown in Figure 3 and Figure 4.

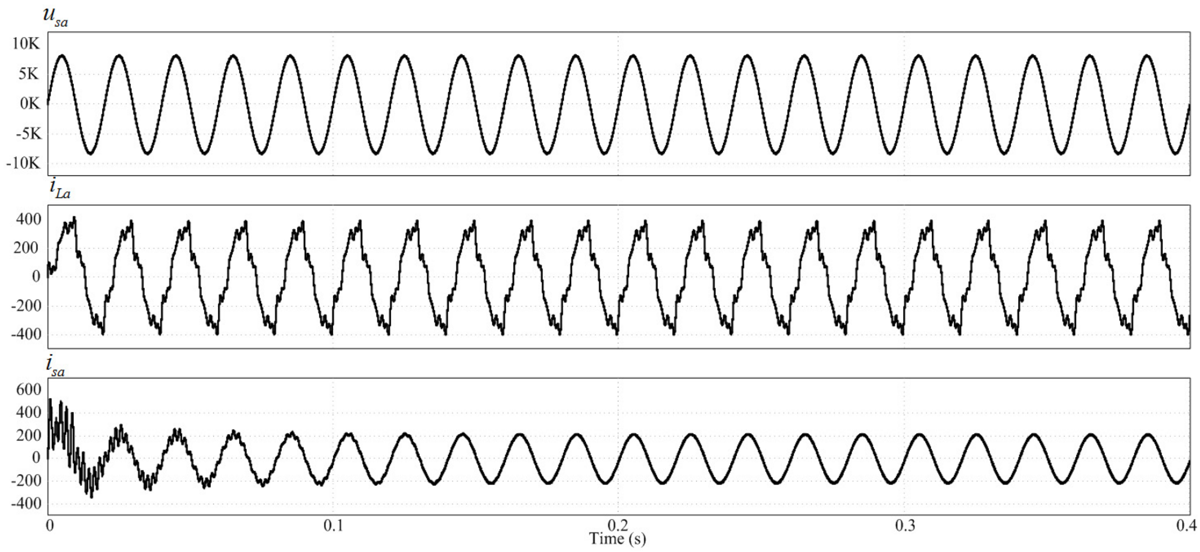

FIGURE 3. Simulation results with the control strategy $U_{inv} = K_1 i_{Lh}$ or $U_{inv} = K_2 i_{sh}$

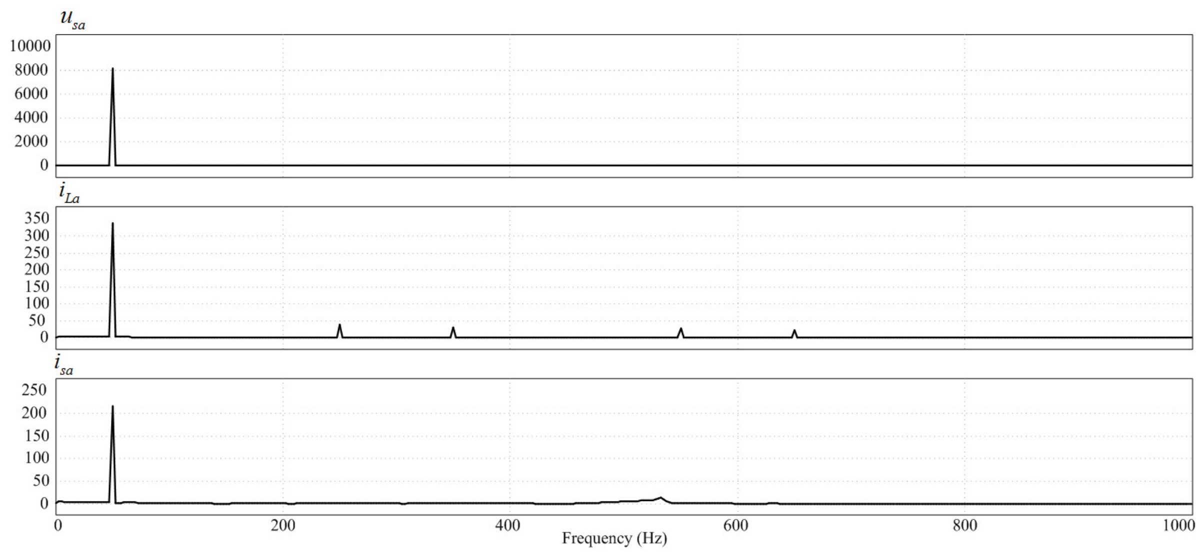

FIGURE 4. Frequency spectrum of waveforms with the control strategy $U_{inv} = K_1 i_{Lh}$ or $U_{inv} = K_2 i_{sh}$

According to Figure 3, when HAPF is not working, the power factor is 0.617, and the total harmonic distortion of the supply current is 17.45%. When HAPF is working (at steady state), the power factor increases to 0.988 from 0.617, the total harmonic distortion of the supply current is 0.552%.

When the source voltage is distorted, the control strategy based on the supply harmonic current gives better results than the control strategy based on the load harmonic current. Simulation results and frequency spectrum of waveforms with the control strategy $U_{inv} = K_1 i_{Lh}$ are shown in Figure 5 and Figure 6.

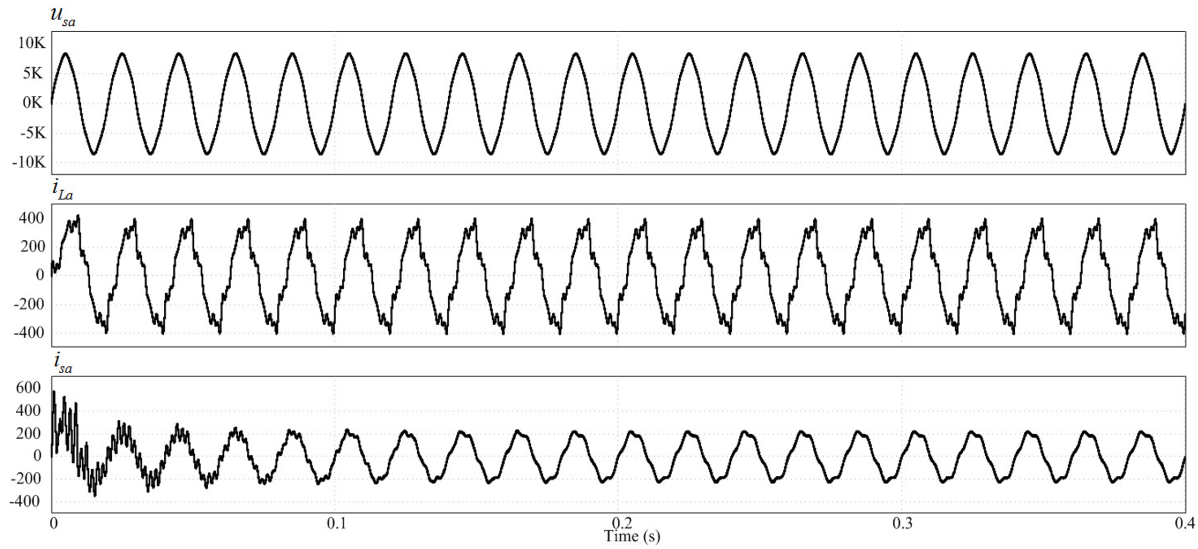

FIGURE 5. Simulation results with the control strategy $U_{inv} = K_1 i_{Lh}$ when the source voltage is distorted

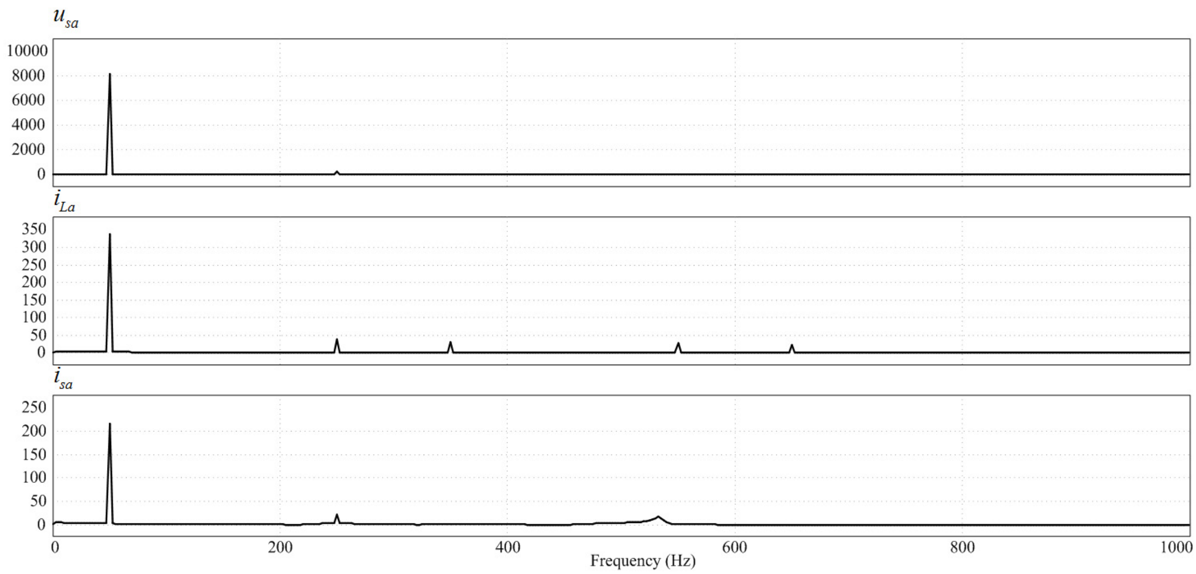

FIGURE 6. Frequency spectrum of waveforms with the control strategy $U_{inv} = K_1 i_{Lh}$ when the source voltage is distorted

According to Figure 5, when HAPF is not connected to the system, the power factor between the source voltage and supply current is 0.617. The total harmonic distortion of the source voltage is 3.056%, and the total harmonic distortion of the supply current is 17.45%. When HAPF is connected to the system (at steady state), the power factor increases to 0.956 from 0.617, and the total harmonic distortion of the supply current is reduced to 10.13% from 17.45%.

The waveforms and frequency spectrums of the source voltage, load current, and supply current with the control strategy based on supply harmonic current are shown in Figure 7 and Figure 8.

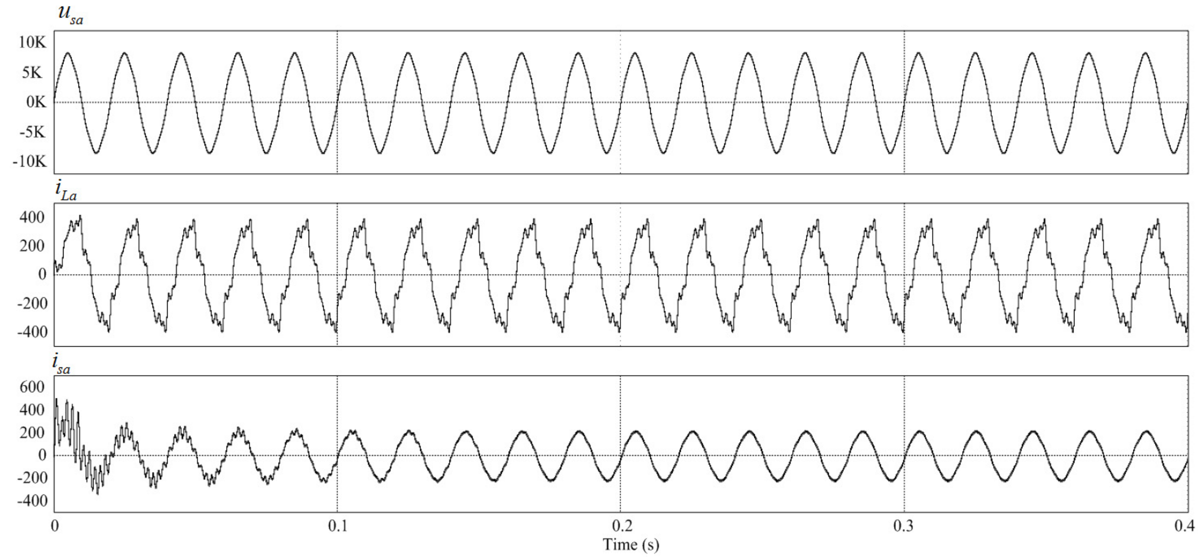

FIGURE 7. Simulation results with the control strategy $U_{inv} = K_2 i_{sh}$ when the source voltage is distorted

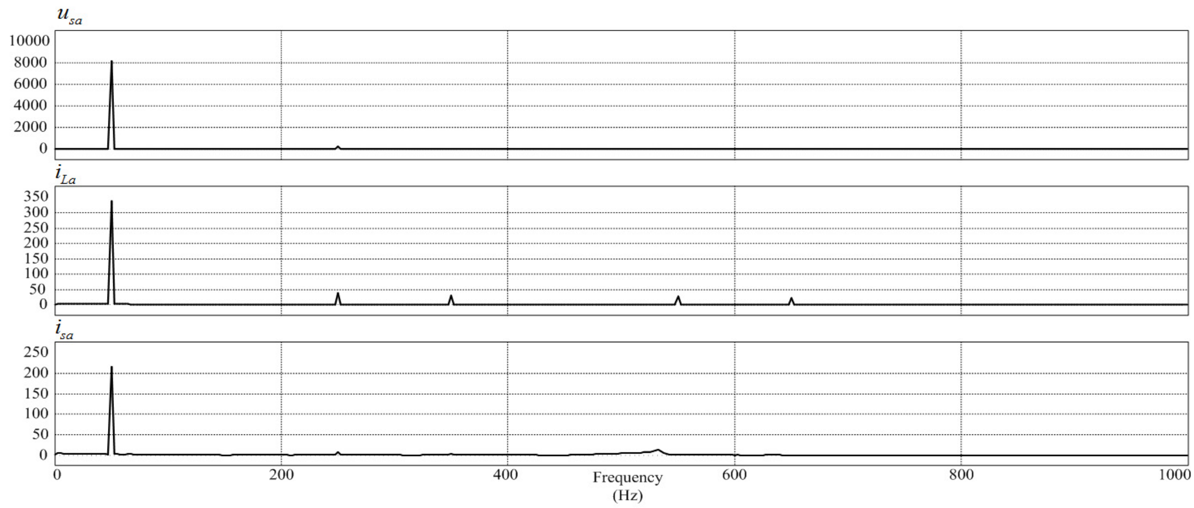

FIGURE 8. Frequency spectrum of waveforms with the control strategy $U_{inv} = K_2 i_{sh}$ when the source voltage is distorted

According to Figure 7, when APF and PPFs are not connected to the system, the power factor between the source voltage and supply current is 0.617 but the total harmonic distortion of the source voltage is 3.056%, and total harmonic distortion of supply current is 17.45%. When APF and PPFs are connected to the system (at steady state), the power factor is 0.966, and the total harmonic distortion of the supply current is reduced to 3.45% from 17.45%.

From the mathematical model and above simulation results, we can see that when the source voltage is distorted, the control strategy based on the supply harmonic current is more effective than the control strategy based on the load harmonic current. However, the control strategy based on the supply harmonic current is also very difficult to cancel most of the harmonic components from the supply current when the source voltage has large distortion.

4. **Conclusions.** The paper analyzed the control mathematical model of HAPF. On that basis, the effectiveness of the control strategies based on the load harmonic current and the supply harmonic current was compared. When the source voltage has no distortion,

the effect of the two above control strategies is the same. When the source voltage has distortion, the control strategy based on supply harmonic current is more effective than the control strategy based on load harmonic current in eliminating harmonic components and preventing resonance. This study will be the basis for finding new control methods for HAPF under non-ideal source conditions.

Acknowledgment. The authors gratefully acknowledge the helpful comments and suggestions of the reviewers, which have improved the presentation.

REFERENCES

[1] B. S. Yogananda and K. Thippeswamy, Design of power filters to improve power quality in power systems, *International Conference on Energy, Communication, Data Analytics and Soft Computing*, pp.1953-1956, 2017.
[2] M. Chau, A. Luo, F. Ma, Z. Shuai, T. Nguyen and W. Wang, Online control method with time-delay compensation for hybrid active power filter with Injection Circuit, *IET Power Electronics*, vol.5, no.8, pp.1472-1482, 2012.
[3] N. Liu, X. Lyu, Y. Zhu and J. Fei, Active disturbance rejection control for current compensation of active power filter, *International Journal of Innovative Computing, Information and Control*, vol.12, no.2, pp.407-418, 2016.
[4] B. R. Madhu et al., Design of shunt hybrid active power filter to reduce harmonics on AC side due to non-linear loads, *International Journal of Power Electronics and Drive System (IJPEDS)*, vol.9, no.4, pp.1926-1936, 2018.
[5] J. Yang, Y. Liu and Z. Li, Unconstrained continuous control set model predictive control based on Kalman filter for active power filter, *International Journal of Innovative Computing, Information and Control*, vol.17, no.5, pp.1705-1716, 2021.
[6] T. K. Truong and C. M. Thuyen, A new flowchart for parameters calculation of Hybrid Active Power Filter with Injection Circuit, *PloS ONE*, vol.16, no.7, pp.1-17, 2021.
[7] C. M. Thuyen, A new approach in design for hybrid active power filter, *ICIC Express Letters*, vol.12, no.9, pp.897-904, 2018.
[8] C. M. Thuyen, A new design algorithm for Hybrid Active Power Filter, *International Journal of Electrical and Computer Engineering (IJECE)*, vol.9, no.6, pp.4507-4515, 2019.
[9] C. V. Bao and C. M. Thuyen, DC-bus voltage stabilization of hybrid active power filter, *ICIC Express Letters*, vol.13, no.1, pp.27-33, 2019.
[10] A. Luo, Z. Shuai, Z. J. Shen, W. Zhu and X. Xu, Design considerations for maintaining DC-side voltage of hybrid active power filter with injection circuit, *IEEE Trans. Power Electronics*, vol.24, no.1, pp.75-84, 2009.
[11] A. Luo, Z. Shuai, W. Zhu, R. Fan and C. Tu, Development of hybrid active power filter based on the adaptive fuzzy dividing frequency-control method, *IEEE Trans. Power Delivery*, vol.24, no.1, pp.424-432, 2009.
[12] C. S. Lam, M. C. Wong and Y. D. Han, Hysteresis current control of hybrid active power filters, *IET Power Electron*, vol.5, no.7, pp.1175-1187, 2012.
[13] Y. Suresh, A. K. Panda and M. Suresh, Real-time implementation of adaptive fuzzy hysteresis band current control technique for shunt active power filter, *IET Power Electronics*, vol.5, no.7, pp.1188-1195, 2012.
[14] A. Luo, X. Xu, H. Fang, H. Fang, J. Wu and C. Wu, Feedback feed forward PI type iterative learning control strategy for hybrid active power filter with injection circuit, *IEEE Trans. Industrial Electronics*, vol.57, no.11, pp.3767-3779, 2010.
[15] C. M. Thuyen, Improved p-q harmonic detection method for Hybrid Active Power Filter, *International Journal of Electrical and Computer Engineering*, vol.8, no.5, pp.2910-2919, 2018.
[16] R. R. Nasyrov and R. I. Aljendy, Comprehensive comparison between hybrid fuzzy-PI and PSO-PI controllers based active power filter for compensation of harmonics and reactive power under different load conditions, *IEEE Conference of Russian Young Researchers in Electrical and Electronic Engineering*, pp.725-730, 2018.
[17] B. A. Abdallah et al., A comparative study and experimental validation on single phase series active power filter control strategies using PI, FLC and sliding mode controllers, *International Journal of Power Electronics and Drive System (IJPEDS)*, vol.10, no.2, pp.731-743, 2019.
[18] S. R. Das, Fuzzy sliding mode based series hybrid active power filter for power quality enhancement, *Advances in Fuzzy Systems*, vol.2018, pp.1-8, 2018.

[19] M. T. Chau, A. Luo, Z. Shuai, F. Ma, N. Xie and V. B. Chau, Novel control method for a hybrid active power filter with injection circuit using a hybrid fuzzy controller, *Journal of Power Electronics*, vol.12, no.5, pp.800-812, 2012.

[20] M. T. Chau, Adaptive current control method for hybrid active power filter, *Journal of Electrical Engineering*, vol.67, no.5, pp.343-350, 2016.

[21] Y.-G. Leu, T.-T. Lee and W.-Y. Wang, On-line tuning of fuzzy-neural network for adaptive control of nonlinear dynamical systems, *IEEE Trans. Systems, Man, and Cybernetics*, vol.27, no.6, pp.1034-1043, 1997.

[22] J. Mazumdar, R. G. Harley and F. C. Lambert, Neural network based method for predicting nonlinear load harmonics, *IEEE Trans. Power Electronics*, vol.22, no.3, pp.1036-1045, 2007.

[23] A. Benyamina, S. Moulahoum, I. Colak and R. Bayindir, Hybrid fuzzy logic-artificial neural network controller for shunt active power filter, *The 5th IEEE International Conference on Renewable Energy Research and Applications (ICRERA)*, pp.837-844, 2016.

[24] M. Jalil and A. Amiri, An effective structure of three-phase parallel hybrid active power filter to accurate harmonic elimination, *The 15th International Conference on Protection and Automation of Power Systems (IPAPS)*, pp.123-129, 2020.

[25] M.-C. Wong, Y. Pang, Z. Xiang, L. Wang and C.-S. Lam, Assessment of active and hybrid power filters under space vector modulation, *IEEE Trans. Power Electronics*, vol.36, no.3, pp.2947-2963, 2021.